PERGAMON

Computers & Graphics 27 (2003) 133–141

COMPUTERS & GRAPHICS

www.elsevier.com/locate/cag

Technical section

On intrinsic representations of 3D polygons for shape blending

Hui Chen, Wenping Wang*

Department of Computer Science and Information Systems, The University of Hong Kong, CYC421, HKU Main Campus, Pokfulam Road, Hong Kong, China

Accepted 18 October 2002

Abstract

An intrinsic representation of a geometric object comprises a set of parameters that are invariant under Euclidean transformations and determine the shape and size of the object uniquely. Unlike the case of a two-dimensional polygon which has essentially only one intrinsic representation, a three-dimensional (3D) polygon allows several variations. We study three different intrinsic representations of a 3D polygon, focusing on properties regarding their applications in shape blending. We show that only one of these representations, which is a natural extension to the intrinsic functions of a 3D differentiable curve, is suitable for shape blending, while the others lead to discontinuous shape transformation. Detailed discussions about the evaluation criteria, numerical sensitivity, and an inherent difficulty in shape blending of 3D polygons are also presented.

Keywords: Morphing; Intrinsic representation; Shape blending; 3D polygon

1. Introduction

Shape representation is an important topic in computer graphics, geometric modeling [1], computational topology [2], computer vision [3], and pattern recognition [4]. A shape representation is a representation from which the shape of a geometric entity can be retrieved. In this paper, we confine ourselves to the study of intrinsic representations of a three-dimensional (3D) polygon. An intrinsic representation of a polygon comprises a set of parameters that are invariant under Euclidean transformations and determine the shape and size of the polygon uniquely, up to a Euclidean transformation, i.e., rotation and translation. More specifically, besides being invariant under Euclidean transformations, an intrinsic representation must be such that (1) two polygons of different shapes or sizes give rise to two different representations; (2) two polygons with the same shape and size, but possibly different positions and orientations, have the same representation.

Let $\Gamma = \{P_i\}_{i=0}^{n}$ denote a 3D polygon of $n+1$ vertices, where $P_i \in E^3$. We call $P_i - P_{i-1}$ the *side vector*, $|P_i - P_{i-1}|$ the *side length*, and $E_i \equiv (P_i - P_{i-1})/|P_i - P_{i-1}|$ the *unit side vector*. The angle between two consecutive side vectors is called a *vertex angle*. Clearly, the side length and vertex angle are invariant under Euclidean transformations. Hence, an intrinsic presentation of a polygon can be defined in terms of these invariant parameters. An intrinsic representation is called a local intrinsic representation if it is defined by the invariant parameters based on the local geometry of a polygon, rather than the global geometry.

One of the applications of intrinsic representations of polygons is shape blending, also known as *shape averaging*, *shape interpolation*, *metamorphosis*, or *morphing* in the literature. A shape blending algorithm takes two objects, called *source objects*, as input, and produces

*Corresponding author. Tel.: +852-2859-7074; fax: +852-2559-8447.

E-mail address: wenping@csis.hku.hk (W. Wang).

0097-8493/03/$ - see front matter
PII: S0097-8493(02)00251-0

a parameterized inbetween object changing continuously from the shape of one source object to the shape of the other. Shape blending has widespread applications in illustration, computer animation, and industrial design [5–7]. In general, the shape concerned can be represented by a two-dimensional (2D) or 3D curve (open or closed) [8,7], a polyhedron [9,10], or a 2D image [11]. A comprehensive literature survey on 3D metamorphosis can be found in [12].

The intrinsic representation of a 2D polygon based on its side lengths and vertex angles is well known and serves as the basis of the shape blending algorithm for 2D polygons in [8]. Although various shape representations, including some intrinsic ones, of 3D polygons, have been proposed for shape blending, there is a lack of systematic study on intrinsic representations of a 3D polygon. Consequently, existing shape blending methods for 3D polygons either do not possess some basic shape preserving properties or do not produce continuous shape transformation in general.

While a 2D polygon has only one local intrinsic representation, a 3D polygon has several different local intrinsic representations that appear to be similar to each other. One of these representations is the discrete generalization of the intrinsic functions of a 3D differentiable curve, i.e., the curvature and torsion in the arclength of the curve. We shall show that this representation produces continuous shape transformation, while the others may cause discontinuity in shape blending.

The remainder of the paper is organized as follows. In Section 2, we review related work and give some preliminaries. In Section 3, three intrinsic representations of 3D polygons are introduced. In Section 4, we study the properties of the acceptable intrinsic representation in the light of its application to shape blending. The paper concludes in Section 5.

2. Related work and preliminaries

Given two source objects Γ^A and Γ^B, the goal of a shape blending algorithm is to transform the shape of Γ^A into that of Γ^B in a continuous and natural manner. There are two major steps in shape blending: *correspondence* and *interpolation*. The correspondence problem concerns establishing a correspondence between features on Γ^A and those of Γ^B [11,13,14]; here the features may be points, line segments, or other geometric entities. Once a correspondence has been obtained, the interpolation problem concerns how features on Γ^A move into their corresponding features on Γ^B, producing a sequence of *inbetween* objects $\Gamma(t)$ from Γ^A to Γ^B, $t \in [0,1]$. Different shape blending methods use different shape representations, and most of these methods perform linear interpolation between the representations of two source objects.

The intrinsic representation of 2D polygons is studied in [8] and used there to devise a shape blending method for 2D polygons. Given a polygon $\Gamma = \{P_i\}_{i=0}^n$, $P_i \in E^2$, this intrinsic representation consists of the side length $\ell_i = |P_i - P_{i-1}|$, $i = 1, 2, \ldots, n$, and the vertex angle between vector $P_i - P_{i-1}$ and vector $P_{i+1} - P_i$, $i = 1, 2, \ldots, n-1$.

A shape interpolation scheme based on an implicit representation of 3D polygons is proposed in [7]. This representation consists of the side lengths and the unit side vectors of the polygon, with a unit side vector represented by a point on S^2. The shape interpolation is carried out by performing a linear interpolation between two corresponding side lengths and a spherical linear interpolation between two corresponding unit side vectors on S^2. Since the unit side vectors are represented in a coordinate-dependent manner, this representation is not intrinsic. As a consequence, the shape transformation produced with this representation is not invariant under Euclidean transformations of input source polygons.

An intrinsic representation of a 3D polygon is proposed in [15] for shape blending. We skip the details of this representation, since it is a particular case of the more general class of local intrinsic representations that we will discuss in the next section. We just point out that the shape blending method proposed in [15] based on this representation does not, in general, produce a continuous shape transformation.

Shape interpolation based on an intrinsic representation entails the following steps: (1) Convert the coordinate representations of the source polygons into intrinsic representations; (2) interpolate the parameters in the intrinsic representations of the source polygons to obtain the intrinsic representation of an inbetween polygon; (3) convert the inbetween intrinsic representation into the coordinate representation of the inbetween polygon.

Stable conversions between the intrinsic representation and the coordinate representation as required above is critical to ensuring smooth shape transformation; however, some degenerate configurations, such as the collinearity of consecutive vertices, make the conversion unreliable or ill-defined. While effective heuristics are available to overcome some of these degeneracies, discontinuous shape transformation becomes unavoidable in the case where two source polygons with no three consecutive vertices being collinear result in an inbetween polygon with three collinear consecutive vertices. More specifically, when converting the Euclidean coordinates to an intrinsic representation of a fixed 3D polygon Γ, a local orthogonal coordinate frame needs to be defined at each vertex so as to specify the position of a vertex using local intrinsic parameters with respect to

its preceding vertices, and such a local coordinate frame is most naturally defined by relative vectors connecting consecutive vertices of the polygon. When three consecutive vertices of the polygon are collinear, such a local frame cannot be defined locally, but can be duplicated from the preceding frame which has been defined. However, in the case of a parameterized inbetween 3D polygon $\Gamma(t) = \{P_i(t)\}_{i=0}^n$, if three consecutive vertices $P_{i-3}(t)$, $P_{i-2}(t)$ and $P_{i-1}(t)$ are collinear at some value $t = t_0$ but otherwise non-collinear in a neighborhood of t_0, then the local frame at $P_{i-1}(t_0)$ is unstable, i.e., it may flip abruptly when the parameter t crosses t_0, and this may result in discontinuous shape transformation. (See more discussions about this in the next section.) Hence, it is necessary to avoid producing collinear consecutive vertices on the inbetween polygon, unless the corresponding vertices on both source polygons are collinear.

3. Three intrinsic representations

In this section, we introduce three different local intrinsic representations of a 3D polygon. Let Γ be a 3D polygon with vertices P_i, $i = 0, 1, \ldots, n$. Denote $Q_i = P_i - P_{i-1}$. The unit side vector is defined by $E_i = Q_i/|Q_i|$. When the three vertices P_{i-1}, P_i, P_{i+1} are not collinear, the normal vector at P_i is $N_i = (Q_i \times Q_{i+1})/|Q_i \times Q_{i+1}|$. When P_{i-1}, P_i and P_{i+1} are collinear, we set N_i equal to N_{i-1}, assuming that the initial normal vector N_0 at vertex P_0 has been specified so as to make this recursive definition valid. In this way, normal vectors at all vertices are well defined.

Given the polygon Γ, the side length $|P_i - P_{i-1}|$ should be chosen as a parameter in an intrinsic representation, since it dictates the size of the polygon. We also need to represent the direction of a side vector $P_i - P_{i-1}$ with respect to its preceding side vector $P_{i-1} - P_{i-2}$. To derive a local representation of this direction, we define a local coordinate system at P_{i-1} spanned by the following three orthogonal vectors: the unit normal vector $R_1 \equiv N_{i-2}$, the unit side vector $R_2 \equiv E_{i-1}$, and their cross product $R_3 \equiv N_{i-2} \times E_{i-1}$. Then we use two angles, longitude and latitude, in spherical coordinates with respect to the frame $\{P_{i-1}; R_1, R_2, R_3\}$ to represent the direction of E_i, which can be identified with a point on S^2 centered at P_{i-1}. A spherical coordinate system is shown in Fig. 1. The Z-axis points to the north pole and the equator plane is determined by the X- and Y-axis.

The following are three natural ways to define a spherical coordinate system with respect to the frame $\{P_{i-1}; R_1, R_2, R_3\}$, by matching up the axes X, Y and Z with the axes R_1, R_2 and R_3, following the right-handed rule. The resulting combinations are: (1) $X = R_1$, $Y = R_2$, $Z = R_3$; (2) $X = R_2$, $Y = R_3$, $Z = R_1$; and (3) $X = R_3$, $Y = R_1$, $Z = R_2$. These are shown in Figs. 2, 3 and 4, respectively. All these three choices give valid local intrinsic shape representations of a 3D polygon with local shape parameters. For the purpose of representing a fixed 3D polygon, one choice is just as good as another. But they exhibit significant difference when applied to blending the shapes of two 3D polygons, as shown by the following analysis.

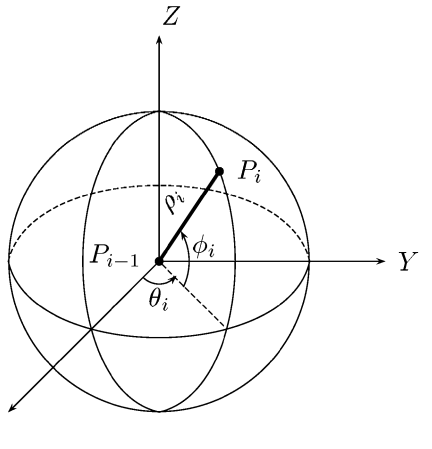

Fig. 1. Spherical coordinates: ρ_i, $\theta_i \in [-\pi, \pi)$, $\phi_i \in [-\pi/2, \pi/2]$.

Choice (1): Referring to Fig. 2, the parameter domain is $(\theta_i, \phi_i) \in [-\pi, \pi) \times [-\pi/2, \pi/2]$. The collinearity of P_{i-2}, P_{i-1} and P_i is characterized by $(\theta_i, \phi_i) = (-\pi/2, 0)$ or $(\theta_i, \phi_i) = (\pi/2, 0)$; P_{i-1} is outside the line segment $P_{i-2}P_i$ when $(\theta_i, \phi_i) = (-\pi/2, 0)$, and P_{i-1} is between P_{i-2} and P_i when $(\theta_i, \phi_i) = (\pi/2, 0)$. That is, both parameter points corresponding to collinearity are interior to the domain $[-\pi, \pi) \times [-\pi/2, \pi/2]$. Since shape interpolation corresponds to linear interpolation in the domain $(\theta_i, \phi_i) \in [-\pi, \pi) \times [-\pi/2, \pi/2]$, the collinearity of three consecutive vertices on an inbetween polygon can occur as the result of interpolating two source polygons with their corresponding vertices being non-collinear. Consequently, a shape blending method based on this choice may produce discontinuous shape transformations, according to the remark at the end of Section 2. This has also been confirmed by our experiments.

Choice (2): Referring to Fig. 3, the parameter domain is again $(\theta_i, \phi_i) \in [-\pi, \pi) \times [-\pi/2, \pi/2]$. The collinearity of P_{i-2}, P_{i-1}, and P_i is characterized by $(\theta_i, \phi_i) = (-\pi, 0)$ or $(\theta_i, \phi_i) = (0, 0)$. Since the point $(\theta_i, \phi_i) = (0, 0)$ is interior to the domain $[-\pi, \pi) \times [-\pi/2, \pi/2]$, the collinearity of three consecutive vertices on an inbetween polygon can again occur as the result of interpolating two source polygons with their corresponding vertices being non-collinear. This choice is made in [15], and the above analysis explains why the shape blending method presented there fails to produce continuous shape transformation in some cases.

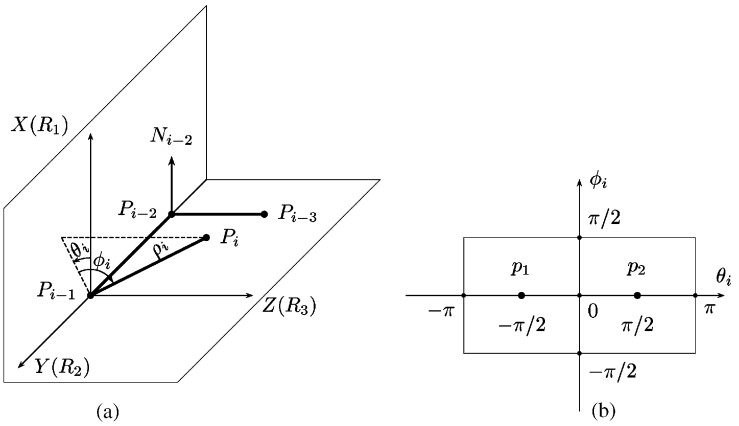

Fig. 2. Choice (1): (a) spherical coordinates; (b) the parameter domain of (θ_i, ϕ_i) and the collinearity points: $p_1 = (-\pi/2, 0)$, $p_2 = (\pi/2, 0)$.

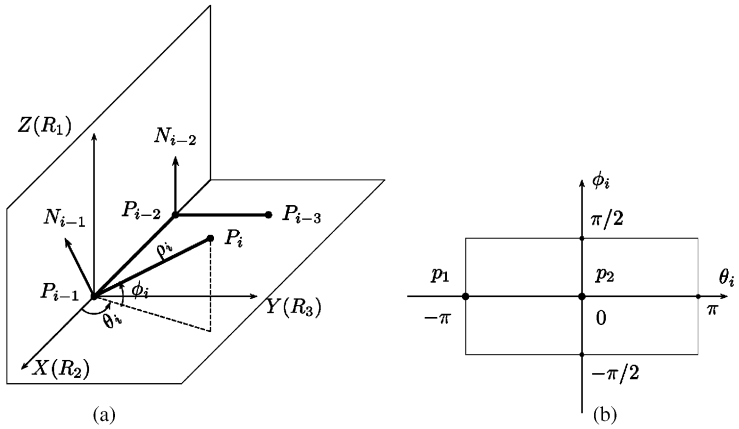

Fig. 3. Choice (2): (a) spherical coordinates; (b) the parameter domain of (θ_i, ϕ_i) and the collinearity points: $p_1 = (-\pi, 0)$, $p_2 = (0, 0)$.

Choice (3): Referring to Fig. 4, the parameter domain is $(\theta_i, \phi_i) \in [-\pi, \pi) \times [0, \pi]$. The collinearity of P_{i-2}, P_{i-1} and P_i is characterized by $\phi_i = 0$ or π. That is, the parameter points (θ_i, ϕ_i) corresponding to collinearity are on two opposite boundary sides of the domain $[-\pi, \pi) \times [0, \pi]$. Since shape interpolation corresponds to linear interpolation within the convex domain $[-\pi, \pi) \times [0, \pi]$ of (θ_i, ϕ_i), if the parameter points of two source polygons are not both on the boundary sides $\phi_i = 0$ or π, then their interpolated parameter point is not on the boundary sides $\phi_i = 0$ or π; that is, the collinearity of three consecutive vertices will not result from two source polygons whose corresponding vertices are non-collinear. We will see in the next section that this intrinsic representation yields continuous shape transformation in shape blending. Since in this choice the side vector E_i is used as the Z-axis vector of the local coordinate system, for the ease of reference, the intrinsic representation based on choice (3) will be called SVN (**S**ide **V**ector for **N**orth) representation, and the corresponding shape blending method will be called the SVN method.

We recap the parameters in the SVN representation in order to facilitate subsequent discussions. Given a polygon Γ with vertices P_i, $i = 0, 1, \ldots, n$, there are three types of intrinsic parameters in the SVN representation of Γ. See Fig. 4. The first is the side length $\ell_i = |P_i - P_{i-1}|$. The second is the angle $\phi_i = \arccos(E_{i-1} E_i) \in [0, \pi]$ between the unit side vectors $E_{i-1} = (P_{i-1} - P_{i-2})/|P_{i-1} - P_{i-2}|$ and $E_i = (P_i - P_{i-1})/|P_i - P_{i-1}|$. The third is the directed angle $\theta_i \in [-\pi, \pi)$ between N_{i-2} and N_{i-1}, with magnitude $|\theta_i| = \arccos(N_{i-2} N_{i-1})$ and sign being the same as the sign of $(P_{i-1} - P_{i-2})(N_{i-2} \times N_{i-1})$. With these parameters, the intrinsic SVN representation of Γ is given by

$$\Omega(\Gamma) \equiv \{\{\ell_i\}_{i=1}^n, \{\phi_i\}_{i=2}^n, \{\theta_i\}_{i=3}^n\}.$$

Clearly, the two shape parameters θ_i and ϕ_i used in the SVN representation are discrete extensions of the

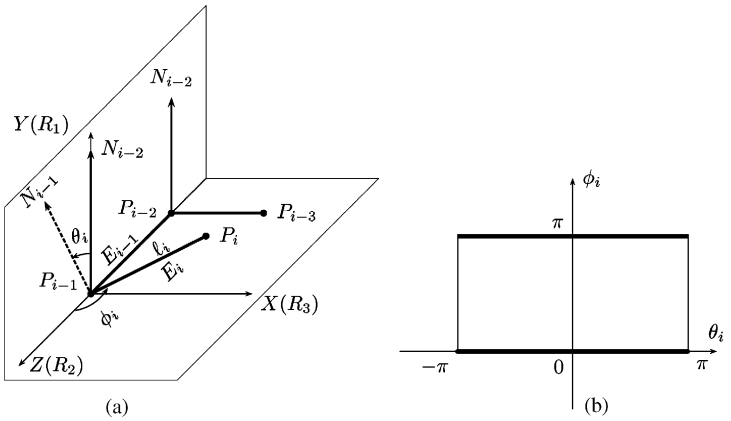

Fig. 4. Choice (3): (a) spherical coordinates; (b) the parameter domain of (θ_i, ϕ_i) and the collinearity on the sides: $\phi_i = 0$, $\phi_i = \pi$.

intrinsic functions of a 3D differentiable curve [16]; θ_i is the angle between two adjacent "osculating" planes and ϕ_i is the angle between two adjacent "tangent lines" (side vectors).

Since an intrinsic representation captures only the shape and size of a polygon, we need to introduce a complete representation to incorporate information about the position and orientation of a polygon, in addition to its shape and size. To this end, we use the first vertex $P_0 = (x_0, y_0, z_0)$, the first unit side vector E_1, and select a normal vector N_0 at P_0, which is perpendicular to E_1; N_0 can be set equal to N_1 or the first properly defined normal vector unless the entire polygon is contained in a straight line. See Fig. 5. A *complete representation* of Γ is thus given by

$$\hat{\Omega}(\Gamma) \equiv \{P_0, O\} \bigcup \Omega(\Gamma), \tag{1}$$

where O is the 3×3 orthogonal matrix $[N_0, E_1, N_0 \times E_1]$.

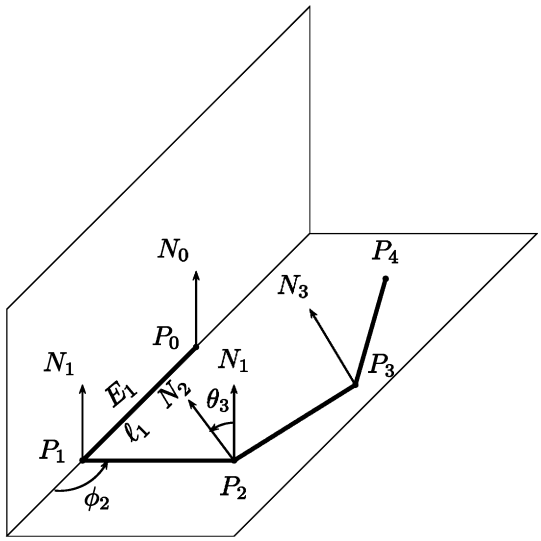

Fig. 5. The setup for the complete representation.

4. Analysis

We have introduced in the last section three intrinsic representations of a 3D polygon, and pointed out that the first two may lead to discontinuous shape transformation. In this section, we concentrate on the third intrinsic representation, called the SVN representation, in the light of its application to shape blending. First, formulas for interpolating intrinsic shape parameters are derived in order to show that the SVN representation ensures the continuity of shape metamorphosis. Then we show that the SVN method satisfies certain basic requirements for shape blending. We also discuss an inherent difficulty in 3D polygon shape blending, which causes the sensitivity of an inbetween polygon to source polygons.

4.1. Interpolation of shape parameters

Let two 3D polygons be given by $\Gamma^A = \{P_i^A\}_{i=0}^n$ and $\Gamma^B = \{P_i^B\}_{i=0}^n$, together with a one-to-one correspondence between the vertices P_i^A and P_i^B. The following three steps are required for producing an inbetween polygon: (1) compute the complete representations $\hat{\Omega}(\Gamma^A)$ and $\hat{\Omega}(\Gamma^B)$; (2) the parameters in $\hat{\Omega}(\Gamma^A)$ and $\hat{\Omega}(\Gamma^B)$ are interpolated to give the inbetween complete representation $\hat{\Omega}(\Gamma(t))$, $t \in [0, 1]$; (3) an inbetween polygon $\Gamma(t)$ is constructed from $\hat{\Omega}(\Gamma(t))$. The first step has

been described in Section 3, so we shall discuss steps 2 and 3 only. Denote the two complete representations by

$$\hat{\Omega}(\Gamma^A) = \{P_0^A, O^A\} \bigcup \Omega(\Gamma^A)$$

where $\Omega(\Gamma^A) = \{\{\ell_i^A\}_{i=1}^n, \{\phi_i^A\}_{i=2}^n, \{\theta_i^A\}_{i=3}^n\}$

and

$$\hat{\Omega}(\Gamma^B) = \{P_0^B, O^B\} \bigcup \Omega(\Gamma^B)$$

where $\Omega(\Gamma^B) = \{\{\ell_i^B\}_{i=1}^n, \{\phi_i^B\}_{i=2}^n, \{\theta_i^B\}_{i=3}^n\}$.

Denote the inbetween polygon at time t by $\Gamma(t)$, and its complete representation by

$$\hat{\Omega}(\Gamma(t)) = \{P_0(t), O(t)\} \bigcup \{\{\ell_i(t)\}_{i=1}^n, \{\phi_i(t)\}_{i=2}^n, \{\theta_i(t)\}_{i=3}^n\}.$$

The parameters in $\hat{\Omega}(\Gamma(t))$ are derived as follows:

$$P_0(t) = (1-t)P_0^A + tP_0^B.$$

The orthogonal matrix $O(t)$ is derived with Slerp interpolation of the unit quaternion presentations of O^A and O^B [17]. Note that $N_0(t)$ and $E_1(t)$ can be extracted from the first two columns of $O(t)$. Further, we have

$$\ell_i(t) = (1-t)\ell_i^A + t\ell_i^B,$$

$$\phi_i(t) = (1-t)\phi_i^A + t\phi_i^B,$$

$$\theta_i(t) = (1-t)\theta_i^A + t\theta_i^B.$$

To ensure that the shortest interpolation path is always used for interpolating $\theta_i(t)$, when it is detected that $|\theta_i^A - \theta_i^B| > \pi$, θ_i^A should be incremented or decremented by 2π so as to make $|\theta_i^A - \theta_i^B| \leqslant \pi$. Although this update moves θ_i^A out of the domain $[-\pi, \pi)$, but it causes no problem in shape interpolation since the intrinsic parameter θ_i has period 2π. We also note that this possible update on θ_i^A and the corresponding expansion of its domain does not affect the analysis in Section 3 on the collinearity of consecutive vertices in the SVN representation.

The next step is to compute the vertices of $\Gamma(t)$ from $\hat{\Omega}(\Gamma(t))$. Initially, with $P_0(t)$, $E_1(t)$ and $N_0(t)$ known, the vertex $P_1(t)$ can be computed as $P_1(t) = P_0(t) + \ell_1(t)E_1(t)$. Suppose that $N_{i-2}(t)$, $E_{i-1}(t)$, and $P_{i-1}(t)$ have been computed, where $i \geqslant 2$. We now wish to compute $P_i(t)$, as well as $N_{i-1}(t)$ and $E_i(t)$. See Fig. 4. Since the angle between $N_{i-1}(t)$ and $N_{i-2}(t)$ is $\theta_i(t)$, we have

$$N_{i-1}(t) = \cos\theta_i(t)N_{i-2}(t) + \sin\theta_i(t)(E_{i-1}(t) \times N_{i-2}(t)). \tag{2}$$

Since $E_{i-1}(t)$ and $E_i(t)$ form angle $\phi_i(t)$ and both lie in the plane with normal vector N_{i-1}, we have

$$E_i(t) = \cos\phi_i(t)E_{i-1}(t) + \sin\phi_i(t)(N_{i-1}(t) \times E_{i-1}(t)). \tag{3}$$

It follows that

$$P_i(t) = P_{i-1}(t) + \ell_i(t)E_i(t). \tag{4}$$

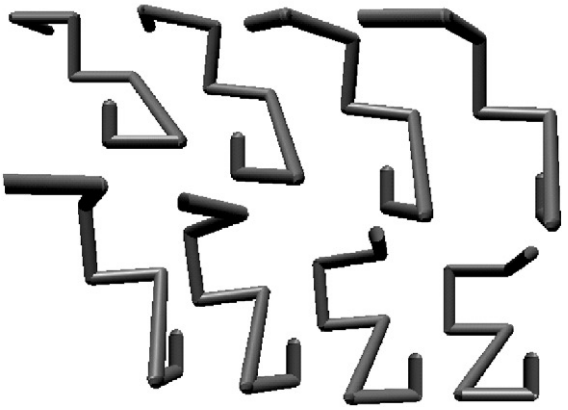

Fig. 6. Shape blending of 3D polygons by the SVN method.

Combining these expressions yields

$$\begin{aligned} P_i(t) = P_{i-1}(t) + \ell_i(t)[&\cos\phi_i(t)E_{i-1}(t) \\ &+ \sin\phi_i(t)\cos\theta_i(t)(N_{i-2}(t) \times E_{i-1}(t)) \\ &+ \sin\phi_i(t)\sin\theta_i(t)N_{i-2}(t)]. \end{aligned} \tag{5}$$

This shows that $P_i(t) - P_{i-1}(t)$ is represented by the spherical coordinates $\ell_i(t)$, $\phi_i(t)$ and $\theta_i(t)$ in the orthonormal frame spanned by the vectors $N_{i-2}(t) \times E_{i-1}(t)$, $N_{i-2}(t)$, and $E_{i-1}(t)$. See Fig. 4. With $N_{i-1}(t)$ and $E_i(t)$ being given above, the subsequent vertices of $\Gamma(t)$ can be computed iteratively.

An example of polygon morphing produced by the SVN representation is shown in Fig. 6. A stick-figure is used here for graphics display, for otherwise the polygons would look too thin to be visible if shown as line segments.

4.2. Criteria for shape blending methods

We now show that the SVN method satisfies the following properties.

Shape continuity: *The inbetween polygon $\Gamma(t)$ is continuous for $t \in [0, 1]$. That is, there is no sudden change of shape, size, position, or orientation during shape blending.*

Identity preserving: *If the source polygons Γ_A and Γ_B are identical in shape, size, position, and orientation, then $\Gamma(t)$ is identical with Γ_A and Γ_B for any $t \in [0, 1]$.*

Shape preserving: *If the source polygons Γ_A and Γ_B have the same shape and size but differ by a rigid motion, then $\Gamma(t)$ also has the same shape and size as Γ_A and Γ_B for any $t \in [0, 1]$. That is, the only difference between $\Gamma(t)$ and Γ_A (or Γ_B) is a rigid motion.*

Feature preserving: *If two corresponding features on the source polygons Γ_A and Γ_B have the same shape and size, then their corresponding feature on $\Gamma(t)$ has the same shape and size for any $t \in [0, 1]$.*

The feature preserving property means that, given two 3D polygons Γ_A and Γ_B, if a part of polygon Γ_A has the same shape and size as its corresponding part on polygon Γ_B, then the shape and size of this part should be preserved in shape blending; thus this property is stronger than the shape preserving property.

Since the intrinsic values ℓ_i, θ_i, and ϕ_i are locally defined, the SVN method has the identity preserving property, the shape preserving property, and the feature preserving property. Below we shall prove that the SVN method has the shape continuity property, i.e., given any two source polygons, the parameterized inbetween polygon $\Gamma(t)$ is continuous in t. In order to speak of shape continuity in this context, we define the metric in the space of 3D polygons of $n+1$ vertices to be

$$d(\Gamma^A, \Gamma^B) = \sum_{i=0}^{n} |P_i^A - P_i^B|$$

for two polygons $\Gamma^A = \{P_i^A\}_{i=0}^n$ and $\Gamma^B = \{P_i^B\}_{i=0}^n$.

We use an inductive argument. It is obvious that the initial position and orientation of $\Gamma(t)$ are continuous in t; that is, $P_0(t)$, $P_1(t)$, $E_1(t)$, and $N_0(t)$ are continuous. Now suppose that $N_{i-2}(t)$, $E_{i-1}(t)$, and $P_{i-1}(t)$ are continuous. Then from formulas (2), (3), and (4), we see that $N_{i-1}(t)$, $E_i(t)$, and $P_i(t)$ are also continuous, since $\theta_i(t)$, $\phi_i(t)$, and $\ell_i(t)$ are continuous. Hence, $\Gamma(t)$ is continuous in t since all its vertices are. This completes the proof of the shape continuity property.

The above four properties can similarly be formulated as criteria for evaluating shape blending methods for other objects. Although these criteria reflect basic and reasonable requirements on shape blending, some existing methods fail to satisfy them. For instance, the shape blending method based on the Minkowski sum for 3D polyhedra in [9] does not have the identity preserving property for non-convex polyhedra. The shape blending method in [7] for 3D polygons does not possess the shape preserving property. The method in [15] for 3D polygons does not possess the shape continuity property.

We note that, the mapping from the geometry of a 3D polygon to its SVN representation is not continuous. The discontinuity, or singularity, occurs when three consecutive vertices of a polygon are collinear. This is illustrated in Fig. 7. Polygon Γ (Fig. 7(a)) has three collinear vertices P_{i-1}, P_i, and P_{i+1}. Perturb P_i to get two slightly different polygons Γ^A and Γ^B in Fig. 7(b), which are identical with Γ except for vertices P_i^A and P_i^B. Vertex P_i^A is on the opposite side of P_i^B in the plane $x=0$. So the normal vectors N_i^A and N_i^B are opposite to each other. Since $\|P_i^A - P_i\| < \delta$ and $\|P_i^B - P_i\| < \delta$ for a sufficiently small value $\delta > 0$, $d(\Gamma^A, \Gamma^B) < 2\delta$. However, for these two polygons we have $\theta_{i+1}^A = 0$ and $\theta_{i+2}^A = 0$, but $\theta_{i+1}^B = -\pi$ and $\theta_{i+2}^B = -\pi$. That is, a small difference between Γ^A and Γ^B gives rise to a big difference in the parameter values of their SVN representations.

Despite this discontinuity in the mapping from polygon geometry to the SVN representation, the inbetween polygon generated by the SVN method is still well behaved and changes its shape continuously, i.e., when two source polygons Γ^A and Γ^B are close to each other, the inbetween polygon $\Gamma(t)$ is also close to Γ^A and Γ^B. That is because this singularity occurs only when three consecutive vertices P_{i-2}, P_{i-1}, and P_i are nearly collinear, in which case we always have $\phi_i \approx 0$ or π, or, equivalently, $\sin\phi_i \approx 0$, which 'scales down' the singularity introduced by θ_i in formula (5) for constructing the inbetween polygon. For the example in

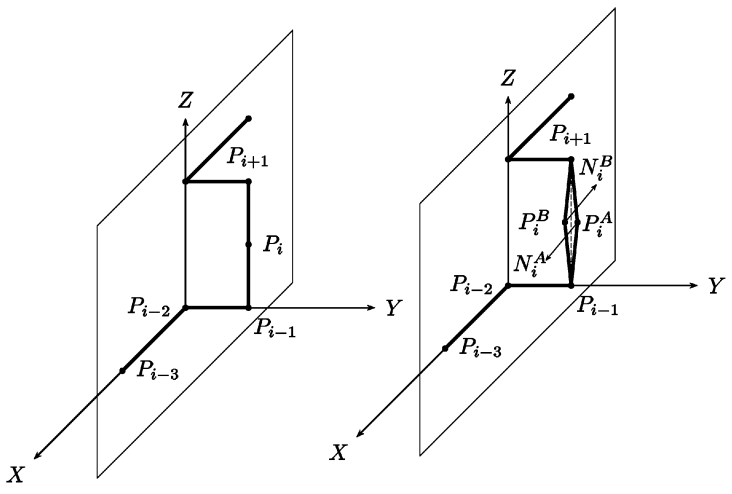

(a) Γ (b) Γ^A and Γ^B

Fig. 7. Mapping discontinuity from geometry to SVN representation.

Fig. 7, $P_i(t)$ rotates around the side $P_{i-1}P_iP_{i+1}$ from P_i^A to P_i^B, while keeping $|P_i(t) - P_{i-1}(t)|$ and $|P_{i+1}(t) - P_i(t)|$ unchanged. That is, the deviation of $P_i(t)$ from the side $P_{i-1}P_iP_{i+1}$ is less than δ for any $t \in [0,1]$. Hence, the shape continuity property is not violated.

4.3. Sensitivity to source polygons

The input to the SVN method consists of two source polygons. The output, or the result of shape blending, is a parameterized inbetween polygon changing continuously from one source polygon to another. We wish to know whether a small change in the source polygons will cause a big difference in the way the inbetween polygon changes its shape. This issue may be regarded as the continuity problem of the mapping from the space of input polygons to the space of output polygon sequences, which should be distinguished from the shape continuity property addressed in Section 4.1.

The output of the SVN method turns out to be sensitive to a perturbation in source polygons in some singular cases. This is illustrated in Fig. 8. Consider polygons $\Gamma = \{A, B, C, D\}$, $\Gamma_1 = \{A, B, C, D_1\}$, $\Gamma_2 = \{A, B, C, D_2\}$, and $\Gamma' = \{A', B', C', D'\}$. When the value of $\delta > 0$ is very small, i.e., $D_1 = (0, 1, -\delta)$ and $D_2 = (0, 1, \delta)$ are both close to $D = (0, 1, 0)$, and Γ_1 and Γ_2 can be thought of as being obtained from Γ through some perturbations. Clearly, using the SVN method, the shape transformation from Γ_1 to Γ' is different from the shape transformation from Γ_2 to Γ', since the sides CD_1 and CD_2 rotate in opposite directions about C towards the side $C'D'$. This means that a small difference between the pair (Γ_1, Γ') and the pair (Γ_2, Γ') causes their respective inbetween polygons to undergo radically different shape transformation processes.

The apparent reason for this is that, although the points D_1 and D_2 are close to each other, their corresponding angle parameters $\theta_{D_1} = \pi - \varepsilon_1$ and $\theta_{D_2} = -\pi + \varepsilon_2$ differ greatly, where $\varepsilon_1 > 0$ and $\varepsilon_2 > 0$ are two small values, while $\theta_{D'} = 0$ for D' on Γ'. So the interpolation from D_1 to D' and the interpolation from D_2 to D' follow different paths as the intrinsic parameter θ is interpolated in different intervals $[0, \pi - \varepsilon_1]$ and $[-\pi + \varepsilon_2, 0]$, respectively, in these two cases. This analysis shows that the sensitivity problem occurs only when a source polygon with one of its θ values near the ends of the parameter domain (i.e., π or $-\pi$) is perturbed.

However, further inspection reveals that this sensitive of the inbetween polygon to source polygons is actually inherent to the shape blending problem of 3D polygons. In the above example, if one wants to change polygon Γ into Γ', while keeping the vertex angle at C unchanged, as required by the shape preserving property, then there are two shortest ways to rotate CD, i.e., either through CD_1 or through CD_2. This ambiguity about which of the two shortest paths the side CD should take cannot be resolved by any shape blending method for 3D polygons that has the shape preserving property. Hence, with the requirement on being shape preserving, the sensitivity problem should not be regarded as a defect of a particular shape blending method for 3D polygons.

5. Conclusion

We have studied the intrinsic representations of a 3D polygon for shape blending of 3D polygons. It is shown that only one of these representations is suitable for shape blending in that it yields continuous shape transformations in all cases. This representation is a natural extension to the intrinsic functions of a differentiable space curve, i.e., the curvature and torsion. Some further properties of this intrinsic representation have been discussed.

It would be an interesting problem to extend the intrinsic representation considered here to the shape blending of skeleton figures which have tree structures in the graph-theoretical sense.

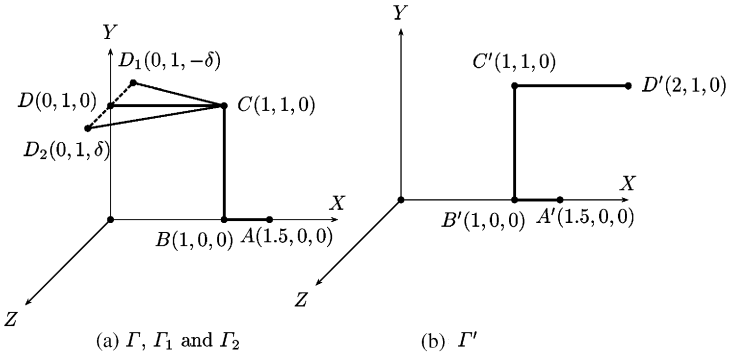

Fig. 8. Sensitivity to source polygons.

Acknowledgements

We would like to thank Prof. Q.S. Peng, Prof. X.G. Jin, and Dr. J.P. Feng for helpful discussions about this research. Thanks also go to Prof. G. Wang for his communications about his research on shape blending.

References

[1] Hoschek J, Lasser D. Fundamentals of computer aided geometric design. A. K. Peters, Ltd., 1993.
[2] Shinagawa Y, Kunii TL, Kergosien YL. Surface coding based on Morse theory. IEEE Computer Graphics and Applications 1991;11(5):66–78.
[3] Haralick RM, Shapiro LG. Computer and robot vision, vol. II. Reading, MA: Addison-Wesley, 1992.
[4] Dryden IL, Mardia KV. Statistical shape analysis. New York: Wiley, 1998.
[5] Catmull E. The problems of computer-assisted animation. Computer Graphics 1978;12(3):348–53.
[6] Sederberg TW, Greenwood E. A physically based approach to 2-D shape blending. Computer Graphics 1992;26(2):25–34.
[7] Peng QS, Jin X, Feng J. Arc-length preserved animation. Computer Animation '97, 1997. p. 86–91.
[8] Sederberg TW, Gao P, Wang G, Mu H. 2-D shape blending: an intrinsic solution to the vertex path problem. Computer Graphics 1993;27(4):15–8.
[9] Kaul A, Rossignac J. Solid-interpolating deformations: construction and animation of PIPs. Proceedings EUROGRAPHICS '91, 1991. p. 493–505.
[10] Kent JR, Carlson WE, Parent RE. Shape transformation for polyhedral objects. Computer Graphics 1992;26(2):47–54.
[11] Beier T, Neely S. Feature-based image metamorphosis. Computer Graphics 1992;26(2):35–42.
[12] Lazarus F, Verroust A. Three-dimensional metamorphosis: a survey. The Visual Computer 1998;14:373–89.
[13] Cohen S, Elber G, Yehuda RB. Matching of free-form curves. Computer Aided Design 1997;29(3):369–78.
[14] Chen SE, Parent RE. Shape averaging and its applications to industrial design. IEEE Computer Graphics and Its Application 1989;9(1):47–54.
[15] Liu L, Wang G. Shape blending between 3-D triangular meshes based on their intrinsic variables, 1998. Preprint.
[16] Carmo M. Differential geometry of curves and surfaces. Englewood Cliffs, NJ: Prentice-Hall, 1976.
[17] Shoemake K. Animating rotation with quaternion curves. Computer Graphics 1985;19(3):15–8.